

# Differential diagnosis of immunoglobulin G4-related sialadenitis and Kimura's disease of the salivary gland: a comparative case series

W.-X. Zhu<sup>1</sup>, Y.-Y. Zhang<sup>1</sup>, Z.-P. Sun<sup>2</sup>,  
Y. Gao<sup>3</sup>, Y. Chen<sup>3</sup>, G.-Y. Yu<sup>1</sup>

<sup>1</sup>Department of Oral and Maxillofacial Surgery, Peking University School and Hospital of Stomatology, National Engineering Laboratory for Digital and Material Technology of Stomatology, Beijing Key Laboratory of Digital Stomatology, Beijing, China; <sup>2</sup>Department of Oral Radiology, Peking University School and Hospital of Stomatology, National Engineering Laboratory for Digital and Material Technology of Stomatology, Beijing Key Laboratory of Digital Stomatology, Beijing, China; <sup>3</sup>Department of Oral Pathology, Peking University School and Hospital of Stomatology, National Engineering Laboratory for Digital and Material Technology of Stomatology, Beijing Key Laboratory of Digital Stomatology, Beijing, China\*\*Address: Yan Chen, Department of Oral Pathology, Peking University School of Stomatology, 22 Zhongguancun South Street, Beijing 100081, China.

W.-X. Zhu, Y.-Y. Zhang, Z.-P. Sun, Y. Gao, Y. Chen, G.-Y. Yu: *Differential diagnosis of immunoglobulin G4-related sialadenitis and Kimura's disease of the salivary gland: a comparative case series*. Int. J. Oral Maxillofac. Surg. 2021; 50: 895–905. © 2020 International Association of Oral and Maxillofacial Surgeons. Published by Elsevier Ltd. All rights reserved.

**Abstract.** The aim of this study was to investigate key points for the differential diagnosis of immunoglobulin G4-related sialadenitis (IgG4-RS) and Kimura's disease (KD) involving the salivary glands. The clinical, serological, radiological, histological, and immunohistochemical features of 85 IgG4-RS cases and 52 KD cases were evaluated comparatively. Seventy-two IgG4-RS cases had enlargement of multiple salivary and/or lacrimal glands; 67 patients had bilateral submandibular gland (SMG) involvement. Unilateral parotid gland involvement (59.6%) and comorbid skin lesions (61.5%) were common in KD. Serum IgG4 was elevated in 94.1% of IgG4-RS cases versus 19.0% of KD cases (cut-off value = 266.5 mg/dl). KD was more commonly associated with elevated eosinophil counts (86% vs 23.1%) and elevated IgE concentrations (95.5% vs 76.6%). Storiform fibrosis, irregular lymphoid follicles, and increased IgG4-positive cells ( $112.9 \pm 37.6$ /high-power field (HPF)) were common in IgG4-RS. Acellular fibrosis, regular lymphoid follicles, IgE-positive reticular networks, increased IgE-positive cells ( $43.4 \pm 26.7$ /HPF), and tryptase-positive mast cells ( $29.7 \pm 13.3$ /HPF) were usually detected in KD. Computed tomography showed that 85.7% of KD cases involved subcutaneous fat tissue. A superficial hypoechoic and reticular pattern with multiple hypoechoic foci were the sonographic features of the SMG in IgG4-RS. Despite numerous overlapping manifestations, histopathological examination showed meaningful differences in the types of fibrosis, eosinophils, and IgG4-positive cell counts. Comprehensive evaluation of clinical, serological, radiological, and histopathological features are crucial for the differential diagnosis.

**Key words:** IgG4-related sialadenitis; IgG4-related diseases; Kimura's disease; immunoglobulin E; salivary gland.

Accepted for publication 6 May 2020  
Available online 29 December 2020

Immunoglobulin G4-related disease (IgG4-RD) is a multi-organ, immune-mediated disease characterized by tumefactive lesions and elevated serum IgG4 concentrations, IgG4-positive plasma cell infiltration, storiform fibrosis, and obliterative phlebitis<sup>1</sup>. As a part of IgG4-RD, IgG4-related sialadenitis (IgG4-RS) is gradually attracting attention. It can affect both the salivary glands and lacrimal glands, and results in gland enlargement with reduced saliva secretion<sup>2,3</sup>.

Kimura's disease (KD, eosinophilic hyperplastic lymphogranuloma) is a chronic lymphoproliferative inflammatory disorder of unknown aetiology<sup>4</sup>, which was first described and compared with Mikulicz's disease by Kimm and Szeto in China in 1937<sup>5</sup>, and was defined and widely known as KD in 1948<sup>6</sup>. It tends to occur among young or middle-aged men, and predominantly involves the regional lymph nodes and salivary glands, with elevated peripheral blood eosinophils (PBE) and serum IgE<sup>7</sup>.

IgG4-RS and KD share many features, including tumefaction of the glands and lymph nodes, elevated PBE and serum IgE levels, histopathological features of lymph follicle hyperplasia, fibrosis, tissue eosinophilia, and increased IgE- and IgG4-positive cell infiltration<sup>2,7-13</sup>. The therapeutic approaches for IgG4-RS include glucocorticoids, conventional steroid-sparing agents<sup>14</sup>, and B cell depletion by rituximab<sup>1</sup>, which contrast starkly with KD. In KD, controversy regarding the optimal treatment exists, and these include surgical excision, radiotherapy, and surgical resection combined with low-dose postoperative radiotherapy; steroid therapy is administered as a second-line treatment<sup>15</sup>. Therefore, the differential diagnosis of these two diseases is essential for optimizing treatment and evaluating the prognosis. Kottler et al. indicated that KD should be differentiated from cutaneous IgG4-RD<sup>12</sup>, and some case reports have found IgG4-positive cells in the lacrimal gland, lymph nodes, and oedematous subcutaneous biopsy specimens in KD<sup>16-18</sup>. However, few studies have focused on the differential diagnosis of IgG4-RS and KD with salivary gland involvement. This study was therefore performed to investigate their clinical, radiographic, serological, histological, and immunohistochemical features, with the aim of establishing clear distinctions between these two diseases.

## Materials and methods

### Patient selection and study design

Eighty-five patients with IgG4-RS diagnosed between August 2011 and December 2018 at the Peking University School of Stomatology were included in this study. The diagnosis was based on the comprehensive diagnostic criteria for IgG4-RD: (1) persistent (>3 months) swelling of single or multiple major salivary glands; (2) serum IgG4 concentration >135 mg/dl; (3) histopathological and immunohistochemistry examinations showing marked lymphocyte and plasmacyte infiltration and fibrosis, as well as infiltration of IgG4-positive plasma cells (IgG4-positive/IgG-positive cell ratio >40% and >50 IgG4-positive plasma cells/high powered field (HPF)); and (4) exclusion of other diseases that present with glandular swellings, such as sarcoidosis and lymphoproliferative disease<sup>19,20</sup>. Eighty cases (94.1%) were diagnosed as definite IgG4-RS and five (5.9%) as probable IgG4-RS. According to the 2019 ACR/EULAR (American College of Rheumatology/European League Against Rheumatism) IgG4-RD classification criteria, all IgG4-RS cases scored >20 points<sup>20</sup>.

Fifty-two patients diagnosed with KD between January 2003 and December 2018 at the Peking University School of Stomatology were selected after standardized histological reappraisal by two expert pathologists and after clinicopathological correlation. The diagnosis of KD was based on previously reported descriptions and criteria: clinically, the presence of a subcutaneous mass occurring preferentially on the head and neck, salivary or lacrimal gland involvement, and elevated blood IgE or eosinophilia; pathologically, the presence of non-lymphomatous lymphoid infiltration with postcapillary venule proliferation, eosinophilia, follicular hyperplasia with well-formed mantle zones, perivenular and stromal sclerosis, proteinaceous deposits in germinal centres (GCs), and eosinophilic microabscesses<sup>7</sup>. All KD cases were diagnosed as definite KD.

The clinical and laboratory data and radiological images of the IgG4-RS and KD cases were reviewed and analysed retrospectively.

### Laboratory examinations

Serological analyses were performed for the total IgG and IgG subclasses in all IgG4-RS cases and 21 KD cases, and for total IgE (T-IgE) in 77 IgG4-RS cases and 22 KD cases. The PBE count was mea-

sured at diagnosis in 78 IgG4-RS cases and 50 KD cases. An elevated eosinophil count was defined as  $>0.5 \times 10^9$  cells/l or >5% leukocytes. In eight KD cases, the T-IgE value exceeded the maximum value of the machine (5000 kU/l) and was recorded as 5000 kU/l.

### Computed tomography (CT) and ultrasonographic image examinations

CT was conducted with an 8-row scanner (BrightSpeed; GE Medical Systems, Waukesha, WI, USA). A biphasic CT protocol was performed, consisting of an unenhanced and enhanced acquisition. The images were then obtained with a scanning delay of 25 seconds. The CT images were analysed by an experienced radiologist and two oral and maxillofacial surgeons who were blinded to the clinical information. Decisions were determined in consensus. Lymph nodes with a long diameter >1.5 cm or a short diameter >0.8 cm were recorded as enlarged<sup>13,21</sup>. Ultrasound examinations were performed using a GE LOGIQ 3 Expert scanner (GE Healthcare, Milwaukee, WI, USA). The transducer frequency was 7–10 MHz. The ultrasonographic images were routinely analysed by an experienced oral radiologist. The imaging features of the two groups were compared.

### Histological examination

All IgG4-RS and KD cases underwent histopathological examination of the salivary glands by incisional or excisional biopsy, and the sections of 45 KD cases were acquired and analysed in this series. The IgG4-RS biopsy tissue included 76 cases involving the submandibular gland (SMG), eight cases involving the parotid gland (PG), and one case of sublingual gland (SLG). The KD biopsy tissue included four cases involving the SMG, 40 cases involving the PG, and one case involving the palatine gland. Two pathologists independently reviewed haematoxylin and eosin-stained slides of all cases according to the diagnostic criteria for IgG4-RS<sup>19</sup> and KD<sup>4,7</sup>. Three HPFs with the greatest eosinophil density were quantified (HPF area = 0.2375 mm<sup>2</sup>). The reporting pathologists graded tissue eosinophil infiltration as none (0), mild (0–25), moderate (25–100), or marked (>100).

### Immunohistochemical examination

Tissue sections (4- $\mu$ m thickness) were deparaffinized and rehydrated. Endoge-

nous peroxidase activity was blocked using 3% H<sub>2</sub>O<sub>2</sub>. Antibodies against human IgG4 (pre-diluted ZA0576; Zhongshan, Beijing, China), IgG (pre-diluted ZA0448; Zhongshan), IgE (pre-diluted ab75673; Abcam, Cambridge, UK), and mast cell tryptase (diluted 1:1000, ab2378; Abcam) were used for immunohistochemical staining. Antigen retrieval was achieved by treating sections with boiling citric acid buffer solution (0.01 mol/l, pH 6.0) for 10 minutes in a microwave oven. Colour was developed using freshly made diaminobenzidine. The sections were washed briefly in running tap water and stained lightly with Mayer's haematoxylin. The expression of IgE-positive cells in the GCs was recorded as none, partial, and entire reticular network. Three identical HPFs with the greatest IgG-, IgG4-, IgE-positive cells outside the GCs and the tryptase-positive mast cell density were quantified using Image-Pro Plus 6.0 (Media Cybernetics, Rockville, MD, USA). Immunohistochemical examination of IgG4 and IgG (85 IgG4-RS and 45 KD specimens), IgE (78 IgG4-RS and 37 KD specimens), and tryptase (67 IgG4-RS and 33 KD specimens) was performed.

### Statistical analyses

The statistical analyses were performed using IBM SPSS Statistics version 20.0 (IBM Corp., Armonk, NY, USA). The mean  $\pm$  standard deviation or median (interquartile range, IQR) was used for continuous variables, and these were compared by independent *t*-test or Wilcoxon rank test. Categorical variables were expressed as percentages and compared using the  $\chi^2$  test or Fisher's exact test. The relationships between the variables were analysed by Pearson correlation test. The sensitivities, specificities, Youden index, and receiver operating characteristics (ROC) curves of serum IgG4, serum T-IgE, PBE, IgG4-positive cells, IgG-positive cells, IgE-positive cells, tryptase-positive mast cells, and tissue IgG4-positive/IgG-positive cell ratios were analysed statistically, and the cut-off value was chosen at the maximum Youden index.  $P < 0.05$  was considered statistically significant.

## Results

### Clinical features

The male to female ratio of the IgG4-RS cases was 0.81:1, which was significantly lower than the ratio in the KD group (7.7:1) ( $P < 0.001$ ). The median age of the IgG4-RS group at diagnosis was 56

Table 1. Clinical features of IgG4-RS and KD cases.

	IgG4-RS (n = 85)	KD (n = 52)	P-value
Male to female ratio	0.81:1	7.7:1	<0.001
Age, years, median (IQR)	56 (50–63)	40 (30–54)	<0.001
Involved glands			
SMG/bilateral SMG, n	83/67	14/5	
PG/bilateral PG, n	44/37	47/16	
SLG/bilateral SLG, n	40/40	2/1	
Multiple gland enlargement, n (%)	72 (84.7)	15 (28.8)	<0.001
Comorbid diseases			
Lymph node enlargement, n (%)	63 (74.1)	49 (94.2)	0.007
Skin symptoms, n (%)	3 (3.5)	32 (61.5)	<0.001
Autoimmune pancreatitis, n (%)	10 (11.8)	0	0.013
Interstitial pneumonia, n (%)	9 (10.6)	0	0.013
Skin nodules of the extremities, n (%)	0	5 (9.6)	0.007
Nephrotic syndrome, n (%)	0	4 (7.7)	0.019
Hypersensitivity diseases, n (%)	55 (64.7)	28 (53.8)	0.258
Allergic rhinitis or asthma, n (%)	39 (45.9)	6 (11.5)	<0.001
Atopic dermatitis or urticaria, n (%)	13 (15.3)	15 (28.8)	0.056
Allergic reactions to drugs and food, n (%)	26 (30.6)	18 (34.6)	0.624

IgG4-RS, immunoglobulin G4-related sialadenitis; IQR, interquartile range; KD, Kimura's disease; PG, parotid gland; SLG, sublingual gland; SMG, submandibular gland.

years (range 9–89 years), which was older than that of the KD group (median 40 years, range 7–77 years) ( $P < 0.001$ ). In the IgG4-RS group, 72 cases (87.2%) had enlargement of multiple glands, and there was bilateral SMG and SLG involvement in 67 and 40 patients, respectively. On palpation, the involved glands were diffusely enlarged and firm. In the KD group, there was salivary gland involvement in all patients, while unilateral gland involvement was more common, especially PG involvement (59.6%) (Table 1). Most KD lesions manifested as a mass with less defined margins involving the skin and subcutaneous tissue, and were soft or toughened on palpation.

Regarding the symptoms, 55 IgG4-RS patients reported symptoms of allergic diseases, including allergic rhinitis or asthma ( $n = 39$ ), atopic dermatitis or urticaria ( $n = 13$ ), and allergic reactions to drugs and food ( $n = 26$ ). Some patients had more than one allergic disease. Systemic comorbidities included autoimmune pancreatitis ( $n = 10$ ) and interstitial pneumonia ( $n = 9$ ). In the KD group, 32 patients had local skin symptoms (pruritus, pachylosis, or pigmentation). The systemic comorbidities of KD included lymph node enlargement or skin nodules of the extremities ( $n = 5$ ), and nephrotic syndrome ( $n = 4$ ).

### Laboratory findings

IgG4-RS patients had significantly higher serum IgG4 and IgG levels than KD patients. Serum IgG4 was elevated in

94.1% of IgG4-RS cases versus 19.0% of KD cases. Compared with IgG4-RS, KD was more commonly associated with elevated eosinophil counts (86% vs 23.1%,  $P < 0.001$ ) and elevated T-IgE concentration (95.5% vs 76.6%,  $P = 0.064$ ). As shown in Table 2, KD patients also had significantly higher serum T-IgE levels and eosinophil counts.

### CT and ultrasonographic imaging characteristics

Thirty IgG4-RS patients showed enlargement of both the bilateral SMG and PG in the CT films (Fig. 1A), which was not seen in any KD patients. In the IgG4-RS group, the CT features of the PG were multiple small nodules (<1 cm diameter) or stripe-like lesions (43.0%) (Fig. 1B), and 31.6% of cases had significant enhancement of the PG peripheral subfascial regions. The involved IgG4-RS SMG had a nodular appearance (40%) (Fig. 1C) and unilateral solitary mass-like lesions (4%). Furthermore, 20.3% of IgG4-RS patients had accessory parotid gland swelling (Fig. 1A). In the KD cases, the CT features of PG were mass-like lesions (64.3%) (Fig. 1D), diffuse hyperdensity of the gland (14.3%) (Fig. 1E), and enhancement of the peripheral subfascial regions (17.9%). Furthermore, the PG enhanced peripheral region in KD was accompanied by subcutaneous fat tissue involvement (Fig. 1D). In the KD patients, the SMG had blurred boundaries with the lymph nodes and platysma (35.7%) (Fig. 1F). Lymphadenopathy was present in 75.9%

Table 2. Serological features of IgG4-RS and KD cases<sup>a</sup>.

	IgG4-RS	KD	P-value
Raised serum IgG4, n (%)	80 (94.1)	4 (19.0)	<0.001
Raised EOS, n (%)	18 (23.1)	43 (86)	<0.001
Raised serum T-IgE, n (%)	59 (76.6)	21 (95.5)	0.064
IgG (g/l), median (IQR)	15.4 (12.3–21.2)	12.0 (11.0–13.4)	<0.001
IgG4 (mg/dl), median (IQR)	552 (227–1340)	102 (54.1–121.5)	<0.001
EOS (%), median (IQR)	2.3 (1.3–4.11)	23.3 (12.4–30.6)	<0.001
T-IgE (kU/l), median (IQR)	371.4 (132–1656)	2790 (1573–5000)	<0.001

EOS, eosinophils; IgG4-RS, immunoglobulin G4-related sialadenitis; IQR, interquartile range; KD, Kimura's disease; T-IgE, total IgE.

<sup>a</sup>Raised EOS  $>0.5 \times 10^9$  cells/l or  $>5\%$  leukocytes; raised serum IgG4  $>135$  mg/dl; raised serum T-IgE  $>100$  kU/l.

of IgG4-RS cases and all KD cases, while unilateral and parotid region lymph node enlargement was more common in KD patients. Sonography also showed different features between IgG4-RS and KD. In the IgG4-RS group, the most prominent sonographic features were a superficial hypoechoic (61.4%) and reticular pattern with multiple hypoechoic foci (35.7%) in the SMG. Regarding KD, the PG showed space-occupying (37.9%) and multiple hypoechoic foci (34.5%) (Table 3).

### Histopathological and immunohistochemical features

Fibrosis is one of the histopathological manifestations in both IgG4-RS and KD. However, its features differ between the two. IgG4-RS patients had storiform fibrosis and periductal collagen sheath (Fig. 2A, C), while KD patients had acellular fibrosis (Fig. 2B) and periductal or perivenular concentric fibrosis (Fig. 2D). Lymphoid follicles could be seen in both

IgG4-RS and KD; the former showed expanded reactive GCs and were usually irregular (Fig. 2A), whereas the latter showed regular GCs (Fig. 2B). Eosinophil infiltration is another histopathological feature of both IgG4-RS and KD, but with differing infiltration pattern and extent. Mild-to-moderate eosinophil infiltration was observed in 63.5% of IgG4-RS cases (median count = 4/HPF), while 66.7% of KD cases had eosinophilic deposits in the GCs. Eosinophilic microabscesses ( $n = 31$ ) and eosinophil-infiltrated neural fibres ( $n = 16$ ) were typical features of KD (Table 4).

Immunohistochemical staining showed elevated IgG4-, IgG-, IgE-, and tryptase-positive cells in both IgG4-RS and KD. In the IgG4-RS group, IgG4-positive cells were widely increased (Fig. 2E), and the IgG4-positive and IgG-positive cell counts, as well as the IgG4-positive/IgG-positive ratios were significantly higher than those in the KD group (Table 5). In the KD group, IgG4-positive cells were distributed focally, mainly in the periductal area and with more severe lymphocyte infiltration (Fig. 2F). In both dis-

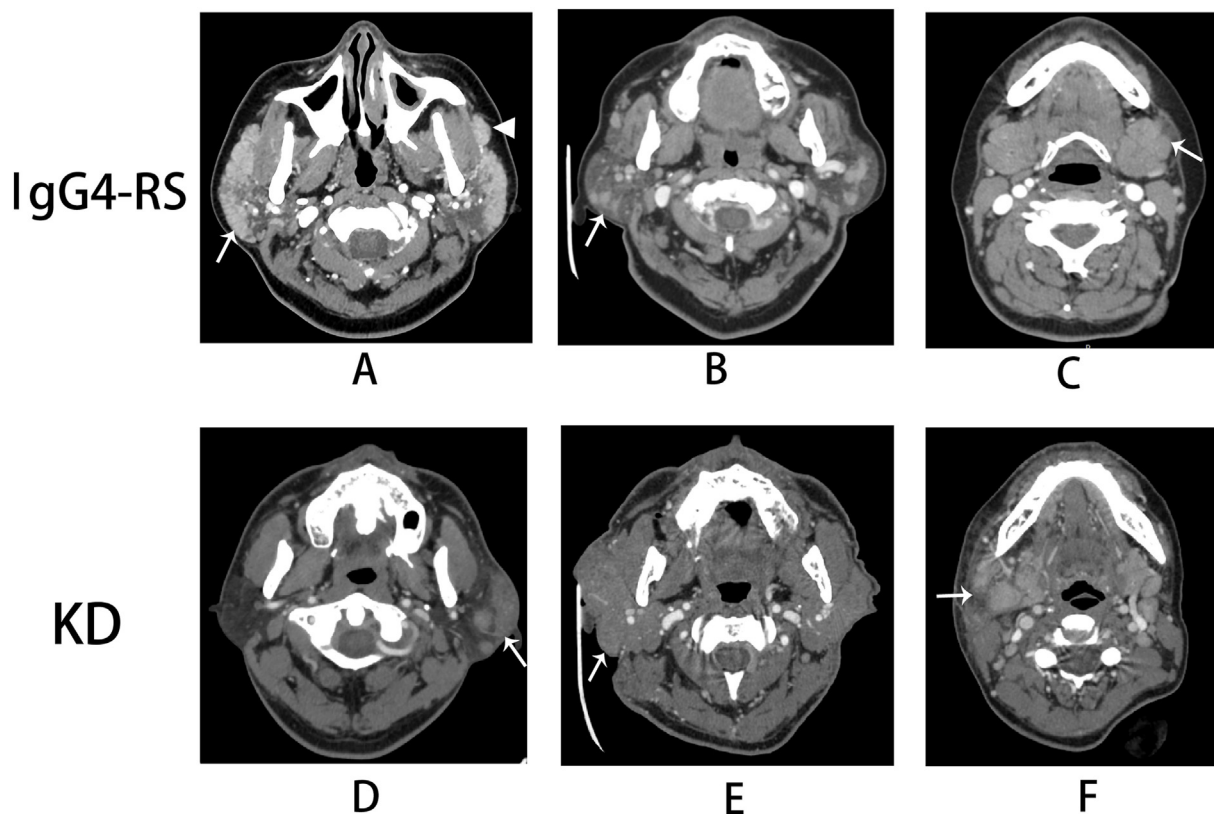


Fig. 1. Axial CT images of patients with immunoglobulin G4-related sialadenitis (IgG4-RS; images A–C) and Kimura's disease (KD; images D–F). (A) Density enhancement of the superficial part of the parotid gland (arrow) and accessory parotid gland (arrowhead). (B) Multiple small nodules (arrow) and stripe-like lesions of the parotid gland. (C) Submandibular gland with a nodular appearance (arrow). (D) Ill-defined patchy-like configuration with well-defined mass-like lesion and subcutaneous fat atrophy in the parotid gland (arrow). (E) Diffuse hyper-density and enlargement of the entire parotid gland (arrow). (F) Ill-defined submandibular gland margins with adjacent tissue structures (arrow).

Table 3. Imaging features of IgG4-RS and KD cases.

	IgG4-RS	KD	P-value
CT imaging features			
SMG			
n = 75	n = 28		
Nodular appearance, n (%)	30 (40)	0	<0.001
Solitary mass-like lesions, n (%)	3 (4)	0	0.565
Blurred boundaries to adjacent tissue, n (%)	4 (5.3)	10 (35.7)	<0.001
PG			
n = 79	n = 28		
Multiple small nodules or stripe-like lesions, n (%)	34 (43.0)	1 (3.6)	<0.001
Diffuse hyperdensity of entire gland, n (%)	5 (6.3)	4 (14.3)	0.364
Mass-like lesion, n (%)	7 (8.9)	18 (64.3)	<0.001
Peripheral subfascial region enhancement, n (%)	25 (31.6)	5 (17.9)	0.163
Subcutaneous fat tissue involvement, n (%)	5 (6.3)	24 (85.7)	<0.001
Lymph node enlargement	60 (75.9)	28 (100)	0.003
Unilateral, n (%)	13 (16.5)	19 (67.9)	<0.001
Bilateral, n (%)	47 (59.5)	9 (32.1)	0.013
Parotid region lymph nodes, n (%)	8 (10.1)	20 (71.4)	<0.001
Sonographic features			
SMG			
n = 70	n = 29		
Superficial hypoechoic, n (%)	43 (61.4)	1 (3.4)	<0.001
Reticular pattern with multiple hypoechoic foci, n (%)	25 (35.7)	0	<0.001
Gland heterogeneity, n (%)	5 (7.1)	4 (13.8)	0.507
Space-occupying, n (%)	2 (2.9)	1 (3.4)	1
PG			
Superficial hypoechoic, n (%)	5 (7.1)	0	0.318
Reticular pattern with multiple hypoechoic foci, n (%)	10 (14.3)	10 (34.5)	0.023
Gland heterogeneity, n (%)	3 (4.3)	5 (17.2)	0.081
Space-occupying, n (%)	2 (2.9)	11 (37.9)	<0.001

IgG4-RS, immunoglobulin G4-related sialadenitis; KD, Kimura's disease; PG, parotid gland; SMG, submandibular gland.

eases, IgE-positive cells were mainly localized in the interfollicular areas and scattered throughout the atrophied acini area with lymphocytic infiltration and fibrosis. However, they showed different features of IgE expression. In IgG4-RS specimens, the IgE-positive staining was either in the surface membrane with ring-like staining or in the cytoplasm (Fig. 2G), and 34.6% of cases had IgE-positive reticular networks in the entire ( $n = 12$ ) or partial ( $n = 15$ ) GCs. In the KD group, there were markedly more IgE-positive cells in the surface membrane than in the cytoplasm, and IgE-positive cells showed typical reticular networks in the GCs (Fig. 2H). Tryptase-positive mast cells were mainly located in the parafollicular areas and the periductal fibrosis area in both diseases, albeit in different quantities. Mast cells were only slightly and focally increased in IgG4-RS (Fig. 2I), while KD specimens had wide mast cell infiltration (Fig. 2J). KD patients had significantly higher IgE-positive and tryptase mast cells than IgG4-RS patients.

In IgG4-RS, serum IgE and tissue IgE-positive cell counts were not correlated, but serum levels of IgE and the tissue tryptase-positive mast cell count were positively correlated ( $r = 0.359$ ,  $P = 0.006$ ). The tissue IgE-positive cell count was significantly correlated with tissue tryptase-positive mast cells in both the IgG4-RS ( $r = 0.318$ ,  $P = 0.009$ ) and KD groups ( $r = 0.514$ ,  $P = 0.003$ ) (Fig. 3).

tase-positive mast cells in both the IgG4-RS ( $r = 0.318$ ,  $P = 0.009$ ) and KD groups ( $r = 0.514$ ,  $P = 0.003$ ) (Fig. 3).

#### Diagnostic testing

In the differential diagnosis of IgG4-RS and KD, when tissue eosinophil counts were <100 cells/HPF, we obtained a good sensitivity of 100% and a specificity of 93.3% for diagnosing IgG4-RS. According to the ROC curve, IgG4-positive cell counts had the best area under the curve (AUC = 0.968) (Fig. 4), and IgG4-positive cells >68/HPF had 87.1% sensitivity and 92.9% specificity (Table 6). Therefore, tissue eosinophil counts and IgG4-positive cell counts performed the best in diagnostic testing. Table 6 also shows that the values of serum IgG4 (>266.5 mg/dl), IgG-positive cell counts (>111.5/HPF), and IgE-positive cell counts (<21/HPF) were meaningful indicators in the diagnosis of IgG4-RS. By comparison, the marked serum IgE elevation (cut-off value = 1817 kU/l) and PBE (cut-off value = 11.6%) were the typical features of KD.

#### Discussion

IgG4-RS and KD are two different entities with different principles of therapy. How-

ever, their clinical and histopathological manifestations, and laboratory evaluations share many similarities, which makes the differential diagnosis difficult. Therefore, clarifying their similarities and differences is critical for diagnosis. For this purpose, we comparatively evaluated the clinical, serological, radiological, histological, and immunohistochemical features of IgG4-RS and KD involving the salivary gland, with large case samples.

This comprehensive study showed many similarities between IgG4-RS and KD. Besides the painless enlargement of the salivary gland and cervical lymph node tumefaction, the similar clinical features include comorbid allergy disease, serum IgE elevation, and peripheral blood eosinophilia. The shared histopathological features are diffuse lymphoplasmacytic infiltration with lymphoid follicle formation, fibrosis, and tissue eosinophilia, as well as the increased IgG4-, IgE-, and tryptase-positive cell infiltration. The overlapping characteristics indicate the possibility that they may have a common aetiological basis, and extrinsic or intrinsic antigens and impaired immune regulation have been implicated as potential aetiological factors of both IgG4-RS<sup>22</sup> and KD<sup>23</sup>. Some researchers, such as Li et al., considered the presence of serum IgG4 elevation and IgG4-positive cell infiltration epiphenomena of KD related to chronic antigen exposure, but several researchers have suggested the co-existence of IgG4-RD and KD<sup>16-18</sup>. The definitive pathogenesis requires further investigation.

Nevertheless, there are obvious differences between the two diseases. In terms of demographic features, the male predominance was very prominent in the KD group, with a male to female ratio of 7.7:1, while no obvious sex difference existed in the IgG4-RS group (0.81:1). Although the age at onset of diagnosis showed a broad age spectrum, the peak age was in the middle-aged or older age group in those with IgG4-RS, while the onset age of KD peaked in the second to fourth decades of life. These results are basically consistent with those of previous studies<sup>1,8,24,25</sup>.

Regarding clinical manifestations, IgG4-RS often involves swelling of multiple exocrine glands, especially the bilateral SMGs, and SLG enlargement is a typical symptom. By contrast, KD is commonly a unilateral lesion and affects the PG. Compared with the bilateral cervical lymph node involvement in IgG4-RS patients, those with KD are subject to ipsilateral lymph node enlargement with

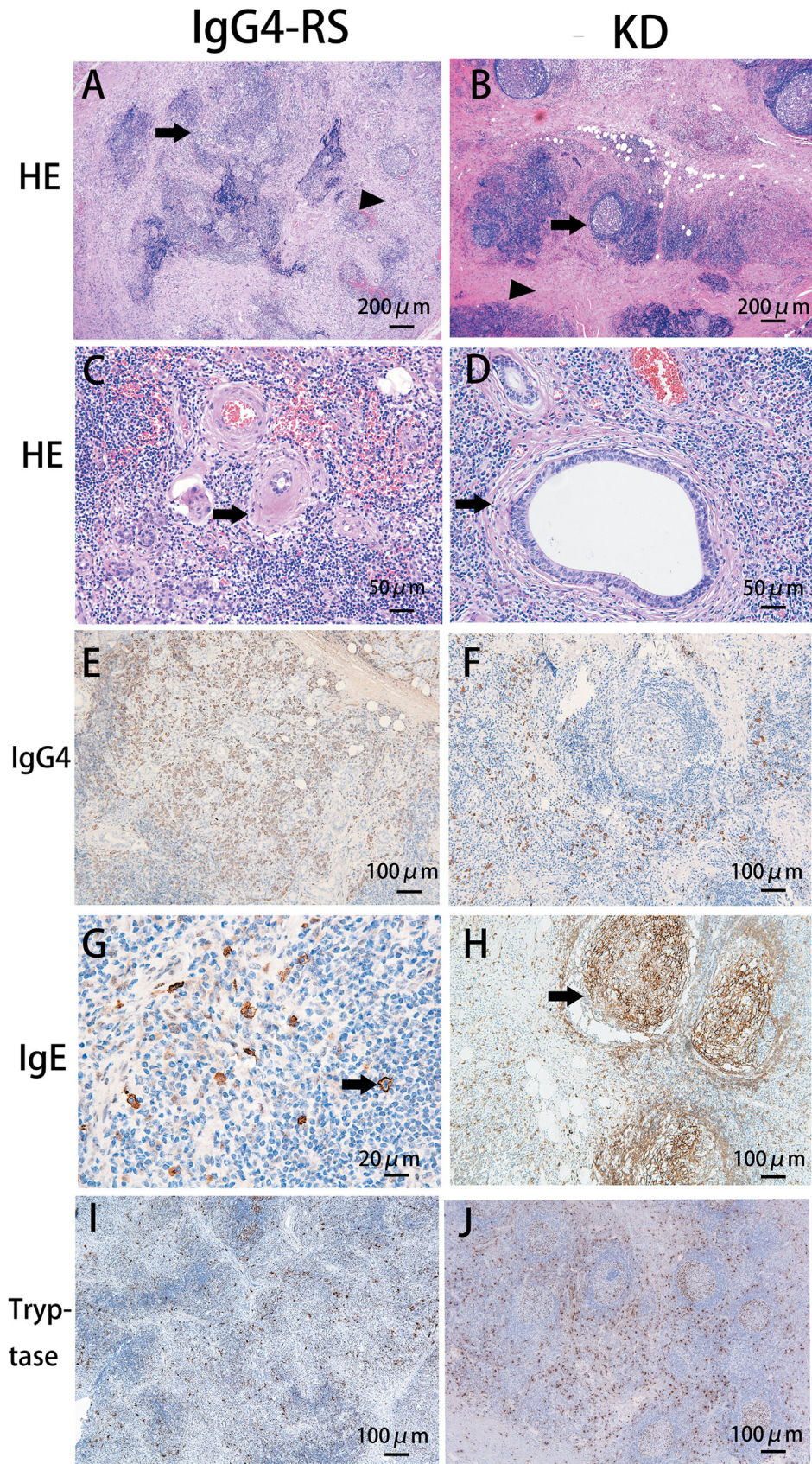


Fig. 2. Histopathological and immunohistochemical features of patients with immunoglobulin G4-related sialadenitis (IgG4-RS; images A, C, E, G, I) and Kimura's disease (KD; images B, D, F, H, J). (A) Storiform fibrosis (arrowhead) and irregular lymphoid follicle formation (arrow) in IgG4-RS. (B) Acellular fibrosis (arrowhead) and regular lymphoid follicle formation (arrow) in KD. (C) Periductal collagen sheath in IgG4-RS

Table 4. Histopathological features of IgG4-RS and KD cases.

	IgG4-RS	KD	P-value
Dense lymphoplasmacytic infiltrate, <i>n</i> (%)	85 (100)	45 (100)	
Regular lymphoid follicle formation, <i>n</i> (%)	0	42 (93.3)	<0.001
Irregular lymphoid follicle formation, <i>n</i> (%)	80 (94.1)	1 (2.2)	<0.001
Acellular fibrosis, <i>n</i> (%)	0	32 (71.1)	<0.001
Storiform fibrosis, <i>n</i> (%)	82 (96.5)	1 (2.2)	<0.001
Concentric circle fibrosis, <i>n</i> (%)	0	34 (75.6)	<0.001
Periductal collagen sheath, <i>n</i> (%)	61 (71.8)	0	<0.001
Eosinophilic deposits in GCs, <i>n</i> (%)	0	30 (66.7)	<0.001
Eosinophilic microabscesses, <i>n</i> (%)	0	31 (68.9)	<0.001
Eosinophil-infiltrated neural fibres, <i>n</i> (%)	0	16 (35.6)	<0.001
EOS (cells/HPF)			
Mild (0–25), <i>n</i> (%)	44 (51.8)	0	
Moderate (25–100), <i>n</i> (%)	10 (11.8)	3 (6.7)	
Marked (>100), <i>n</i> (%)	0	42 (93.3)	

EOS, eosinophils; GC, germinal centre; HPF, high-power field; IgG4-RS, immunoglobulin G4-related sialadenitis; KD, Kimura's disease.

Table 5. Immunohistochemical features of IgG4-RS and KD cases.

	IgG4-RS	KD	P-value
IgG-positive (cells/HPF)	162.7 ± 46.7	63.1 ± 22.4	<0.001
IgG4-positive (cells/HPF)	112.9 ± 37.6	31.0 ± 22.4	<0.001
IgG4-positive/IgG-positive ratio (%)	69.6 ± 13.5	48.5 ± 21.1	<0.001
IgE-positive (cells/HPF)	7.6 ± 7.6	43.4 ± 26.7	<0.001
IgE-positive reticular networks in GCs, <i>n</i> (%)	27 (34.6)	37 (100)	<0.001
IgE-positive networks in entire GCs, <i>n</i> (%)	12 (15.4)	36 (97.3)	
IgE-positive networks in partial GCs, <i>n</i> (%)	15 (19.2)	1 (2.7)	
Tryptase-positive mast cells (cells/HPF)	10.0 ± 5.3	29.7 ± 13.3	<0.001

GC, germinal centre; HPF, high-power field; IgG4-RS, immunoglobulin G4-related sialadenitis; KD, Kimura's disease.

a unilateral lesion, and it is believed that KD lesions in the PG are spread from the intraparotid lymph nodes<sup>4</sup>. In the present series, only 3.5% of IgG4-RS cases presented skin symptoms, and the most common IgG4-related skin diseases are erythematous papules, with a low occurrence rate<sup>1,26</sup>, while pruritus of the lesion skin is the main complaint in KD, which might be caused by eosinophil infiltration into the nerve fibres<sup>4,12</sup>. IgG4-RS patients usually tended to have comorbid allergic rhinitis or asthma (45.9%), while atopic dermatitis or urticaria (28.8%) was common in the KD group. Some clinicians even consider non-specific dermatitis a systemic sign of KD<sup>12</sup>.

Analysis from the perspective of radiology, according to the present findings, showed that the CT appearances of the affected PGs varied and often featured peripheral subfascial region enhancement in the IgG4-RS group, with rare involvement of the subcutaneous fat tissue. Meanwhile, subcutaneous fat tissue involvement in CT imaging was a more

frequent manifestation in KD. It has been speculated that the hyper-enhancement of the PG peripheral subfascial regions in KD is spread from the adjacent subcutaneous tissues and overlying skin<sup>4</sup>. Similar to the sonographic imaging results in the literature<sup>27,28</sup>, a superficial hypo-echoic and reticular pattern with multiple hypoechoic foci of SMG were typical characteristics in IgG4-RS, which differed greatly from the normal pattern of SMG and the space-occupying feature of the PG in KD.

Histopathologically, the storiform fibrosis and irregular lymphoid follicle formation of IgG4-RS, and the marked eosinophil infiltration of KD were the foremost features in the differential diagnosis. IgG4-RS generally showed diffusely increased IgG4-positive cells, as opposed to the focal aggregates of IgG4-positive cells in KD. In IgG4-RS, 19.2% of cases showed IgE-positive reticular network staining merely in light areas of partial GCs, which may be related to the GC degeneration and obscurity of light areas during lesion development<sup>2</sup>. Most

KD cases had strongly and diffusely expressed IgE in the follicular dendritic cells (FDC) within the entire GC. Histopathological features, including the type of fibrosis and GCs, degree of eosinophil infiltration, and tissue IgG4-positive, IgG-positive, and IgE-positive cell counts, are priorities for the differential diagnosis.

In this study, the tryptase-positive mast cells in both diseases were approximately in accordance with the distribution of the IgE-positive cells, especially the surface membrane IgE-positive cells. Evidence of IgE-positive mast cells has been demonstrated in IgG4-RD and KD tissue in previous reports<sup>11,29,30</sup>. The co-staining suggested that membrane IgE-positive cells represent IgE attachment to the mast cells, and the cytoplasmic IgE-positive cells might be IgE-producing B cells or the mast cells through the endocytosis-mediated cytoplasmic accumulation of IgE<sup>11,31</sup>. Subsequently, the chronic elevation of antigen-independent IgE with cytokinergic activity upregulates the IgE receptor on mast cells, which inhibits mast

(arrow). (D) Concentric circle perivenular fibrosis in KD (arrow). (E) Widely increased IgG4-positive cells in IgG4-RS. (F) Focally distributed IgG4-positive cells in KD. (G) Scattered IgE-positive cells with cytoplasm or surface membrane staining (arrow) in IgG4-RS. (H) IgE-positive reticular networks in the germinal centres (arrow) and widely increased IgE-positive cells in KD. (I) Tryptase-positive mast cells distributed in the fibrosis area of IgG4-RS. (J) Widely distributed tryptase-positive mast cells in the parafollicular areas of KD. (HE, haematoxylin-eosin.)

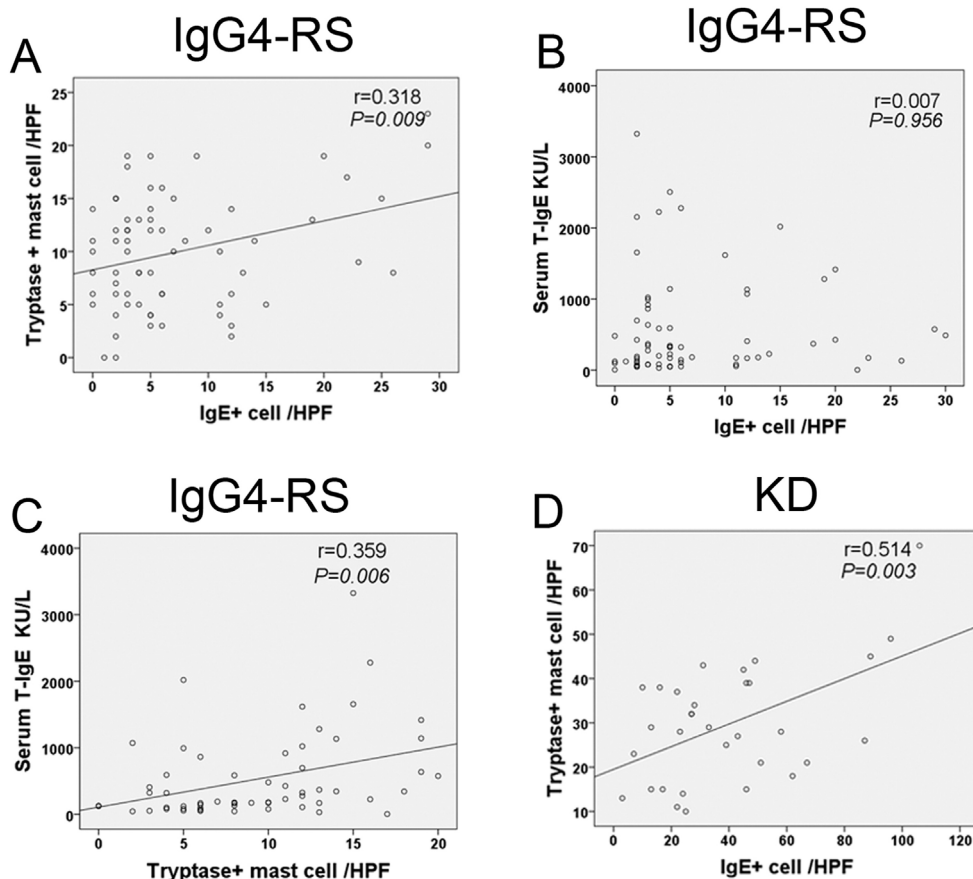


Fig. 3. Correlation plots of the relationships of serum total IgE (T-IgE), tissue IgE-positive cells, and tryptase-positive mast cells in immunoglobulin G4-related sialadenitis (IgG4-RS) and Kimura's disease (KD). (A) Positive correlation between tryptase-positive mast cells and tissue IgE-positive cells in IgG4-RS. (B) No significant correlation between serum T-IgE and tissue IgE-positive cells in IgG4-RS. (C) Positive correlation between serum T-IgE and tryptase-positive mast cells in IgG4-RS. (D) Positive correlation between tryptase-positive mast cells and tissue IgE-positive cells in KD.

cell apoptosis<sup>32</sup>. It has been suggested that increased IgE-positive activated mast cells may play crucial roles in driving the fibrosis in IgG4-RS<sup>31</sup>, and in regulating IgE synthesis and orchestrating eosinophilic infiltration in KD<sup>23,30</sup>. Furthermore, there were different immunological aspects between IgG4-RD and KD. CD4+ cytotoxic T lymphocytes but not CD4+GATA3+ Th2 cells synthesize interleukin (IL)-1 $\beta$  and transforming growth factor (TGF)- $\beta$ 1, suggesting the fibrosis mechanisms in IgG4-RD patients<sup>33,34</sup>. In contrast, the CD4+GATA3+ T cells are present in the affected tissues in KD<sup>30</sup>.

According to the ROC curve, the IgG4-positive cell count is a more powerful tool than the IgG4-positive/IgG-positive ratio in the differential diagnosis with KD, because of the better AUC, which is opposite to the consensus statement for establishing the diagnosis of IgG4-RS<sup>35</sup>. The IgG4-positive/IgG-positive ratio cut-off value was 52.35%, which is higher than the 40% in the

diagnostic criteria<sup>19</sup>. Our preliminary results revealed that tissue eosinophilia (>100/HPF) is of vital importance in diagnosing KD. The IgE-positive and tryptase-positive cell counts contribute to the accuracy of the differential diagnosis. The results of this study are in keeping with the consensus that IgG4-RD diagnosis is based primarily on the morphological appearance and tissue IgG4-positive and IgE-positive cell counts, and that the IgG4-positive/IgG-positive ratio is of secondary importance in the histopathological diagnosis<sup>35</sup>. Besides, serum IgG4 (cut-off value = 266.5 mg/dl) remained an excellent diagnostic indicator. These quantitative findings add substantially to the current knowledge on the differential diagnosis of these two diseases. The key points for the differential diagnosis between the two diseases are summarized in Table 7.

This study has some limitations. First, the study was retrospective in nature, which means that the serological, CT,

and ultrasonographic imaging and immunohistochemical data could not be obtained for all of the patients. Second, double immunohistochemical staining to confirm the IgE-positive mast cells and the common cytokines in the two diseases was not performed, which might have provided more insight into the mechanisms of the overlapping features.

In conclusion, many overlapping manifestations exist in IgG4-RS and KD, and comprehensive evaluation of their clinical, serological, radiological, histopathological, and immunopathological features could provide important clues to their differential diagnosis. The similarity of these two diseases suggests that their pathogenesis might share common factors, but further studies are necessary.

#### Competing interests

All the authors have declared that no conflict of interest exists.

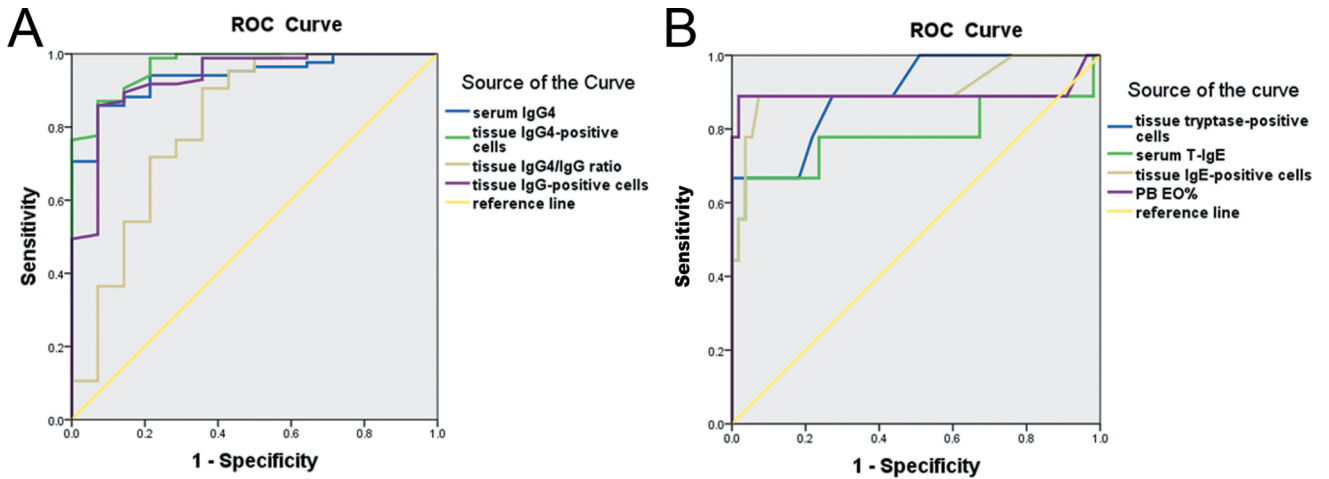


Fig. 4. Receiver operating characteristics (ROC) curves for distinguishing immunoglobulin G4-related sialadenitis (IgG4-RS) and Kimura’s disease (KD). (A) ROC curve of serum IgG4, tissue IgG4-positive cells, IgG-positive cells, and IgG4-positive/IgG-positive ratio. (B) ROC curve of serum total IgE (T-IgE), tissue tryptase-positive cells, IgE-positive cells, and percentage of eosinophils in the peripheral blood (PB EO%).

Table 6. AUC, cut-off value, Youden index, sensitivity and specificity for distinguishing IgG4-RS from KD.

	AUC	95% CI	Cut-off value	Youden index	Sensitivity (%)	Specificity (%)	P-value
IgG4-positive (cells/HPF)	0.968	0.930–1.00	>68	0.799	87.1	92.9	<0.001
IgG4 (mg/dl)	0.938	0.886–0.99	>266.5	0.798	86.9	92.9	<0.001
IgG-positive (cells/HPF)	0.933	0.862–1.00	>111.5	0.787	85.9	92.9	<0.001
IgE-positive (cells/HPF)	0.907	0.767–1.00	<21	0.816	88.9	92.7	<0.001
Tryptase-positive (cells/HPF)	0.898	0.786–1.00	<20.5	0.667	66.7	100	<0.001
EOS (%)	0.894	0.702–1.00	<11.6	0.871	88.9	98.2	<0.001
IgG4-positive/IgG-positive (%)	0.81	0.663–0.958	>52.35	0.549	90.6	64.3	<0.001
T-IgE (kU/l)	0.784	0.558–1.00	<1817	0.63	66.7	96.4	0.007

AUC, area under the receiver operating characteristics curve; CI, confidence interval; EOS, eosinophils; HPF, high-power field; IgG4-RS, immunoglobulin G4-related sialadenitis; KD, Kimura’s disease; T-IgE, total IgE.

Table 7. Conclusions—key points for the differential diagnosis.

	IgG4-RS	KD
Clinical features	Mostly involves bilateral SMG Multiple gland enlargement Comorbid with allergic rhinitis or asthma	Mostly involves unilateral gland PG and lymph node enlargement Comorbid with skin lesions
Serology	Prominent serum IgG4 elevation (>266.5 mg/dl)	Markedly elevated serum IgE (>1817 kU/l) and PBE (>11.6%)
CT imaging	Nodular appearance of enlarged SMG Multiple small nodules or stripe-like lesion of PG Bilateral lymph node enlargement	Subcutaneous fat tissue involvement Mass-like lesion of PG Unilateral and parotid region lymph node enlargement
Ultrasonographic imaging	Superficial hypoechoic and reticular pattern with multiple hypoechoic foci of SMG	Space-occupying and multiple hypoechoic foci of PG
Histopathology	Storiform fibrosis, irregular lymph follicle formation Mild to moderate EOS infiltration	Acellular fibrosis, regular lymph follicle formation Marked EOS infiltration and eosinophilic microabscesses
Immunohistochemistry	Periductal collagen sheath Widely increased IgG4-positive cells (>68/HPF) Slightly increased IgE-positive cells and mast cells	Concentric circle periductal fibrosis Focally and slightly increased IgG4-positive cells Significantly increased IgE-positive cells (>21/HPF) and tryptase-positive mast cells (>21/HPF), and IgE-positive reticular networks in GCs

CT, computed tomography; EOS, eosinophils; GC, germinal centre; HPF, high-power field; IgG4-RS, immunoglobulin G4-related sialadenitis; KD, Kimura’s disease; PBE, peripheral blood eosinophils; PG, parotid gland; SMG, submandibular gland.

## Funding

This work was supported by the National Natural Science Foundation of China (No. 81671005, 81974151, 82081240420).

## Ethical approval

Ethical approval was obtained from the Biomedical Institutional Review Board of Peking University School of Stomatology (PKUSSIRB-201947099).

## Patient consent

Not required.

## Statement to confirm

All co-authors have viewed and agreed to the submission.

## References

- Kamisawa T, Zen Y, Pillai S, Stone JH. IgG4-related disease. *Lancet* 2015;**385**:1460–71. [http://dx.doi.org/10.1016/s0140-6736\(14\)60720-0](http://dx.doi.org/10.1016/s0140-6736(14)60720-0).
- Li W, Chen Y, Sun ZP, Cai ZG, Li TT, Zhang L, Huang MX, Hua H, Li M, Hong X, Su JZ, Zhang ZY, Liu YY, He J, Li ZG, Gao Y, Yu GY. Clinicopathological characteristics of immunoglobulin G4-related sialadenitis. *Arthritis Res Ther* 2015;**17**:186. <http://dx.doi.org/10.1186/s13075-015-0698-y>.
- Yamamoto M, Yajima H, Takahashi H, Yokoyama Y, Ishigami K, Shimizu Y, Tabeya T, Suzuki C, Naishiro Y, Takano K, Yamashita K, Hashimoto M, Keira Y, Honda S, Abe T, Suzuki Y, Mukai M, Himi T, Hasegawa T, Imai K, Shinomura Y. Everyday clinical practice in IgG4-related dacryoadenitis and/or sialadenitis: results from the SMART database. *Mod Rheumatol* 2015;**25**:199–204. <http://dx.doi.org/10.3109/14397595.2014.950036>.
- Gao Y, Chen Y, Yu GY. Clinicopathologic study of parotid involvement in 21 cases of eosinophilic hyperplastic lymphogranuloma (Kimura's disease). *Oral Surg Oral Med Oral Pathol Oral Radiol Endod* 2006;**102**:651–8. <http://dx.doi.org/10.1016/j.tripleo.2005.11.024>.
- Kimm HT, Szeto C. Eosinophilic hyperplastic lymphogranuloma, comparison with Mikulicz's disease. *Chin Med J* 1937;**23**:699–700.
- Kimura T, Yoshimura S, Ishikawa E. On the unusual granulation combined with hyperplastic changes of lymphatic tissue. *Trans Soc Pathol Jpn* 1948;**37**:179–80.
- Chen H, Thompson LD, Aguilera NS, Abbondanzo SL. Kimura disease: a clinicopathologic study of 21 cases. *Am J Surg Pathol* 2004;**28**:505–13.
- Liu Y, Xue M, Wang Z, Zeng Q, Ren L, Zhang Y, Zhang S, Wang Y, Shen D, Xia C, Yu G, Li ZG. Salivary gland involvement disparities in clinical characteristics of IgG4-related disease: a retrospective study of 428 patients. *Rheumatology (Oxford)* 2020;**59**:634–40. <http://dx.doi.org/10.1093/rheumatology/kez280>.
- Wang M, Zhang P, Lin W, Fei Y, Chen H, Li J, Zhang L, Zheng W, Li Y, Zeng X, Zhou J, Lai Y, Liu X, Xue H, Cui Y, Zhou L, Zhao J, Zhang W. Differences and similarities between IgG4-related disease with and without dacryoadenitis and sialoadenitis: clinical manifestations and treatment efficacy. *Arthritis Res Ther* 2019;**21**:44. <http://dx.doi.org/10.1186/s13075-019-1828-8>.
- Della Torre E, Mattoo H, Mahajan VS, Caruthers M, Pillai S, Stone JH. Prevalence of atopy, eosinophilia, and IgE elevation in IgG4-related disease. *Allergy* 2014;**69**:269–72. <http://dx.doi.org/10.1111/all.12320>.
- Culver EL, Sadler R, Bateman AC, Makuch M, Cargill T, Ferry B, Aalberse R, Barnes E, Rispens T. Increases in IgE, eosinophils, and mast cells can be used in diagnosis and to predict relapse of IgG4-related disease. *Clin Gastroenterol Hepatol* 2017;**15**:1444–52. <http://dx.doi.org/10.1016/j.cgh.2017.02.007>.
- Kottler D, Barete S, Quereux G, Ingen-Housz-Oro S, Fraitag S, Ortonne N, Deschamps L, Rybojad M, Flageul B, Crickx B, Janin A, Bagot M, Battistella M. Retrospective multicentric study of 25 Kimura disease patients: emphasis on therapeutics and shared features with cutaneous IgG4-related disease. *Dermatology* 2015;**231**:367–77. <http://dx.doi.org/10.1159/000439346>.
- Hong X, Sun ZP, Li W, Chen Y, Gao Y, Su JZ, Wang Z, Cai ZG, Li TT, Zhang L, Liu XJ, Liu YY, He J, Li ZG, Yu GY. Comorbid diseases of IgG4-related sialadenitis in the head and neck region. *Laryngoscope* 2015;**125**:2113–8. <http://dx.doi.org/10.1002/lary.25387>.
- Hong X, Zhang YY, Li W, Liu YY, Wang Z, Chen Y, Gao Y, Sun ZP, Peng X, Su JZ, Cai ZG, Zhang L, He J, Ren LM, Yang HY, Li ZG, Yu GY. Treatment of immunoglobulin G4-related sialadenitis: outcomes of glucocorticoid therapy combined with steroid-sparing agents. *Arthritis Res Ther* 2018;**20**:12. <http://dx.doi.org/10.1186/s13075-017-1507-6>.
- Ye P, Wei T, Yu GY, Wu LL, Peng X. Comparison of local recurrence rate of three treatment modalities for Kimura disease. *J Craniofac Surg* 2016;**27**:170–4. <http://dx.doi.org/10.1097/SCS.0000000000002337>.
- Liu L, Chen Y, Fang Z, Kong J, Wu X, Zhang Z. Kimura's disease or IgG4-related disease? A case-based review. *Clin Rheumatol* 2015;**34**:385–9. <http://dx.doi.org/10.1007/s10067-013-2462-5>.
- McKelvie PA, Lyons B, Barnett G, Allen PW. Kimura's disease in two Caucasians, one with multiple recurrences associated with prominent IgG4 production. *Pathology* 2012;**44**:275–8. <http://dx.doi.org/10.1097/PAT.0b013e3283513f95>.
- Li J, Ge X, Ma J, Li M, Li J. Kimura's disease of the lacrimal gland mimicking IgG4-related orbital disease. *BMC Ophthalmol* 2014;**14**:158. <http://dx.doi.org/10.1186/1471-2415-14-158>.
- Umehara H, Okazaki K, Masaki Y, Kawano M, Yamamoto M, Saeki T, Matsui S, Yoshino T, Nakamura S, Kawa S, Hamano H, Kamisawa T, Shimosegawa T, Shimatsu A, Nakamura S, Ito T, Notohara K, Sumida T, Tanaka Y, Mimori T, Chiba T, Mishima M, Hibi T, Tsubouchi H, Inui K, Ohara H. Comprehensive diagnostic criteria for IgG4-related disease (IgG4-RD), 2011. *Mod Rheumatol* 2012;**22**:21–30. <http://dx.doi.org/10.1007/s10165-011-0571-z>.
- Wallace ZS, Naden RP, Chari S, Choi H, Della-Torre E, Dicaire JF, Hart PA, Inoue D, Kawano M, Khosroshahi A, Kubota K, Lanzillotta M, Okazaki K, Perugino CA, Sharma A, Saeki T, Sekiguchi H, Schleinitz N, Stone JR, Takahashi N, Umehara H, Webster G, Zen Y, Stone JRH, American College of Rheumatology/European League Against Rheumatism IgG4-Related Disease Classification Criteria Working Group. The 2019 American College of Rheumatology/European League Against Rheumatism classification criteria for IgG4-related disease. *Arthritis Rheumatol* 2020;**72**:7–19. <http://dx.doi.org/10.1002/art.41120>.
- Mancuso AA, Harnsberger HR, Muraki AS, Stevens MH. Computed tomography of cervical and retropharyngeal lymph nodes: normal anatomy, variants of normal, and applications in staging head and neck cancer. Part I: normal anatomy. *Radiology* 1983;**148**:709–14. <http://dx.doi.org/10.1148/radiology>.
- Della-Torre E, Lanzillotta M, Doglioni C. Immunology of IgG4-related disease. *Clin Exp Immunol* 2015;**181**:191–206. <http://dx.doi.org/10.1111/cei.12641>.
- Ohta N, Fukase S, Suzuki Y, Ito T, Yoshitake H, Aoyagi M. Increase of Th2 and Tc1 cells in patients with Kimura's disease. *Auris Nasus Larynx* 2011;**38**:77–82.
- Wang L, Zhang P, Zhang X, Lin W, Tang H, Li J, Wang M, Liu X, Fei Y, Chen H, Peng L, Zhang L, Lai Y, Zeng X, Li X, Xue H, Zhao Y, Zhang F, Zhang W. Sex disparities in clinical characteristics and prognosis of immunoglobulin G4-related disease: a prospective study of 403 patients. *Rheumatology (Oxford)* 2019;**58**:820–30. <http://dx.doi.org/10.1093/rheumatology/key397>.
- Li TJ, Chen XM, Wang SZ, Fan MW, Semba I, Kitano M. Kimura's disease: a clinicopathologic study of 54 Chinese patients. *Oral Surg Oral Med Oral Pathol Oral Radiol Endod* 1996;**82**:549–55.
- Ikeda T, Oka M, Shimizu H, Hatakeyama M, Kanki H, Kunisada M, Tsuji G, Morinobu A,

- Kumagai S, Azumi A, Negi A, Nishigori C. IgG4-related skin manifestations in patients with IgG4-related disease. *Eur J Dermatol* 2013;**23**:241–5. <http://dx.doi.org/10.1684/ejd.2013.1958>.
27. Li W, Xie XY, Su JZ, Hong X, Chen Y, Gao Y, Zhang ZY, Yu GY. Ultrasonographic features of immunoglobulin G4-related sialadenitis. *Ultrasound Med Biol* 2016;**42**:167–75. <http://dx.doi.org/10.1016/j.ultrasmed-bio.2015.09.014>.
28. Shimizu M, Okamura K, Kise Y, Takeshita Y, Furuhashi H, Weerawanich W, Moriyama M, Ohyama Y, Furukawa S, Nakamura S, Yoshiura K. Effectiveness of imaging modalities for screening IgG4-related dacryoadenitis and sialadenitis (Mikulicz's disease) and for differentiating it from Sjögren's syndrome (SS), with an emphasis on sonography. *Arthritis Res Ther* 2015;**17**:223. <http://dx.doi.org/10.1186/s13075-015-0751-x>.
29. Takeuchi M, Ohno K, Takata K, Gion Y, Tachibana T, Orita Y, Yoshino T, Sato Y. Interleukin 13-positive mast cells are increased in immunoglobulin G4-related sialadenitis. *Sci Rep* 2015;**5**:7696. <http://dx.doi.org/10.1038/srep07696>.
30. Maehara T, Munemura R, Shimizu M, Kakiyama N, Kaneko N, Murakami Y, Masafumi M, Kiyoshima T, Kawano S, Nakamura S. Tissue-infiltrating immune cells contribute to understanding the pathogenesis of Kimura disease: a case report. *Medicine (Baltimore)* 2019;**98**:e18300. <http://dx.doi.org/10.1097/MD.00000000000018300>.
31. Takeuchi M, Sato Y, Ohno K, Tanaka S, Takata K, Gion Y, Orita Y, Ito T, Tachibana T, Yoshino T. T helper 2 and regulatory T-cell cytokine production by mast cells: a key factor in the pathogenesis of IgG4-related disease. *Mod Pathol* 2014;**27**:1126–36. <http://dx.doi.org/10.1038/modpathol.2013.236>.
32. Suzuki R, Scheffel J, Rivera J. New insights on the signaling and function of the high-affinity receptor for IgE. *Curr Top Microbiol Immunol* 2015;**388**:63–90. [http://dx.doi.org/10.1007/978-3-319-13725-4\\_4](http://dx.doi.org/10.1007/978-3-319-13725-4_4).
33. Mattoo H, Mahajan VS, Maehara T, Deshpande V, Della-Torre E, Wallace ZS, Kulikova M, Drijvers JM, Daccache J, Carruthers MN, Castellino FV, Stone JR, Stone JRH, Pillai S. Clonal expansion of CD4(+) cytotoxic T lymphocytes in patients with IgG4-related disease. *J Allergy Clin Immunol* 2016;**138**:825–38. <http://dx.doi.org/10.1016/j.jaci.2015.12.1330>.
34. Liu H, Perugino CA, Ghebremichael M, Wallace ZS, Montesi SB, Stone JH, Pillai S. Disease severity is linked to an increase in autoantibody diversity in IgG4-related disease. *Arthritis Rheumatol* 2020;**72**:687–93. <http://dx.doi.org/10.1002/art.41140>.
35. Deshpande V, Zen Y, Chan JK, Yi EE, Sato Y, Yoshino T, Kloppel G, Heathcote JG, Khosroshahi A, Ferry JA, Aalberse RC, Bloch DB, Brugge WR, Bateman AC, Carruthers MN, Chari ST, Cheuk W, Cornell LD, Fernandez-Del Castillo C, Forcione DG, Hamilos DL, Kamisawa T, Kasashima S, Kawa S, Kawano M, Lauwers GY, Masaki Y, Nakanuma Y, Notohara K, Okazaki K, Ryu JK, Saeki T, Sahani DV, Smyrk TC, Stone JR, Takahira M, Webster GJ, Yamamoto M, Zamboni G, Umehara H, Stone JRH. Consensus statement on the pathology of IgG4-related disease. *Mod Pathol* 2012;**25**:1181–92. <http://dx.doi.org/10.1038/modpathol.2012.72>.

Address:  
Guang-yan Yu  
Department of Oral and Maxillofacial  
Surgery  
Peking University School of Stomatology  
22 Zhongguancun South Street  
Beijing 100081  
China  
Tel: +86 10 82195245;  
Fax: +86 10 62173402  
E-mails: 1554326447@qq.com,